C. R. Chimie 15 (2012) 714–718

Contents lists available at SciVerse ScienceDirect

Comptes Rendus Chimie

www.sciencedirect.com

Full paper/Mémoire

A simplistic one-pot method to produce magnetic graphene-CdS nanocomposites

Chengfeng Zhou [a], Zonghua Wang [a,*], Jianfei Xia [a], Brian K. Via [b], Feifei Zhang [a], Yanzhi Xia [a,*], Yanhui Li [a]

[a] *Laboratory of Fiber Materials and Modern Textile, the Growing Base for State Key Laboratory, College of Chemical and Environment Engineering, Qingdao University, Qingdao, 266071 Shandong, China*

[b] *Biomaterials Laboratory, School of Forestry and Wildlife Science, Auburn University, Auburn, 36849 Alabama, United States*

ARTICLE INFO

Article history:
Received 29 March 2012
Accepted after revision 29 May 2012
Available online 12 July 2012

Keywords:
Graphene
Fe_3O_4
CdS
Solvothermal
Nanocomposites

ABSTRACT

A simple, yet novel process was developed where magnetic graphene-CdS (Fe_3O_4-CdS/G) nanocomposites were prepared by a one-pot solvothermal route in which the reduction of graphite oxide (GO) into graphene was accompanied by the generation of CdS and Fe_3O_4 nanoparticles. The results of TEM and XRD studies indicate the formation of Fe_3O_4-CdS/G nanocomposites. Besides vibration sample magnetometry, fluorescence spectra and loading of doxorubicin (DOX) reveal that this new nanocomposite possesses good superparamagnet (44.85 emu/g), good fluorescent properties and a high loading efficiency (0.98 mg/mg). The efficient, stable, and water soluble nanocomposites are confirmed to be suitable for biomedical applications.

© 2012 Published by Elsevier Masson SAS on behalf of Académie des sciences.

1. Introduction

A major challenge to successful cancer chemotherapy has focused on the development of nanoscale tumor-targeted delivery systems. For efficient drug action, improving the drug loading efficiency is critical in drug carrier research. Nanomaterial development and delivery methods are necessary to fight tumors and other biotechnological problems. Graphene is one material that has a two-dimensional plane and consequently a large specific surface area. High surface areas are beneficial and assist in the immobilization of a large number of substances including a wide range of metals, biomolecules, fluorescent molecules, drugs, etc. For example, Yang et al. have found that some anticancer drugs with aromatic systems can be loaded onto graphite oxide (GO) with high efficiency [1]. Dai et al. have demonstrated that the functionalized graphene are biocompatible yet non-toxic and this has resulted in successful drug delivery [2].

On the other hand, site-directed drug targeting is also very important for improving drug efficiency while decreasing the side effects. One promising methodology is to load the magnetic nanoparticles with GO. For instance, decorating magnetic Fe_3O_4 NPs on GO gives Fe_3O_4@GO with promising use in various areas of biology and biomedicine [3]. More recently, a number of researchers have reported preparation of GO@Fe_3O_4 including high temperature decomposition of the precursor $Fe(acac)_3$ on GO [4], ion exchange and subsequent calcinations [5], attachment of Fe_3O_4 to GO through covalent bonding [6], adding $FeCl_3$ to a hot mixture of NaOH and diethylene glycol [7], hydrothermal technique [8] and chemical precipitations [9]. However, a common limitation of drug delivery systems is the lack of an intrinsic signal for long-term and real-time imaging of drug transport. This problem has been partially addressed by conjugation with organic fluorophores. Nonetheless, the photobleaching problem associated with essentially all organic dyes (including fluorescent proteins) prevents long-term tracking or imaging. In this context, quantum

* Corresponding authors.
E-mail addresses: wang_zonghua@yahoo.com.cn (Z. Wang), qdxyzh@163.com (Y. Xia).

1631-0748/$ – see front matter © 2012 Published by Elsevier Masson SAS on behalf of Académie des sciences.
http://dx.doi.org/10.1016/j.crci.2012.05.022

dots (QDs), a new type of fluorescent labeling material, have obtained tremendous attention in high throughput biodetection and cellular imaging techniques [10]. Indeed, they have been used to label both organic and inorganic drug carriers and potentially even bacteria and viruses, with a burst of activity in the area of oligonucleotide (ODN) and siRNA delivery [11]. Currently, the research of preparation graphene – QD nanocomposites has attracted great interests from scientists. For example, Cao et al. have synthesized graphene – CdS nanocomposites by a one-step method in dimethyl sulfoxide (DMSO) [12]. Feng et al. have reported on the preparation of graphene nanosheets decorated with tiny CdS QDs by a facile approach via the π–π stacking interaction using benzyl mercaptan as the interlinker [13]. More recently, Chang et al. synthesized hybrids containing graphene and CdS QDs by in situ growth of CdS QDs on noncovalently functionalized graphene [14].

Most of the nanocomposites so far were only designed as monofunctional drug carriers, and the processes of preparation are complex rendering it impractical for in field use. Also, the reports about the production of multifunctional carriers based on graphene by simple method are limited, so it is necessary to develop a simpler method to synthesize much more efficient multifunctional carriers. Herein, we have developed a novel drug delivery system by multifunctional graphene with Fe_3O_4 and CdS QDs simultaneously through a one-pot solvothermal reaction. The resulting Fe_3O_4-CdS/G nanocomposites possess both the fluorescent and superparamagnetic properties while maintaining good dispersibility in water. Compared with the other common drug carrier materials [15], the Fe_3O_4-CdS/G nanocomposites have a higher loading efficiency. The combined properties of Fe_3O_4-CdS/G holds promise in the fields of controlled targeted drug delivery and fluorescent imaging.

2. Experimental

2.1. Preparation of graphite oxide (GO)

All chemicals and reagents used for experiments and analysis were of analytical grade and purchased from Hefei Bomei Biotechnology Co. Ltd., China. Graphene was synthesized from expandable graphite (Qingdao Henglide Graphite Co., Ltd., China) by a modified Hummers method [16]. Expandable graphite (5 g) was mixed with a mixture of 230 mL sulfuric acid (98%), potassium permanganate (30 g) and sodium nitrate (5 g) in a beaker which was located in an ice bath. The beaker was then removed from the ice bath and the obtained mixture was kept at 0 °C for 24 h. Later on, the mixture was stirred at 35 °C for 30 min and then slowly diluted with deionized water. The reaction temperature was rapidly increased to 98 °C and kept for 15 min. Subsequently, 30% H2O2 (50 mL) was slowly added to the mixture and the color of the mixture changed to bright yellow. After that, the mixture was centrifuged (centrifugation speed 4000 rpm) and washed with HCl (5%) and deionized water several times. After filtration and drying at 25 °C for 3 days, graphene oxide (GO) was obtained.

2.2. Synthesis of Fe_3O_4-CdS/G nanocomposites

Fig. 1 shows a schematic diagram for the formation of Fe_3O_4-CdS/G nanocomposites. First, PSS (0.1 g) was mixed with GO (0.05 g) and stirred for 2 hours then centrifuged, a mixture of GO decorated with PSS was obtained. Next, the modified GO, $CdCl_2$ (0.5 g), $FeCl_2{\cdot}4H_2O$ (0.5 g) and sodium acetate (2.0 g) were dispersed in DMSO (50 mL) solution by vigorous stirring to form a stable suspension until the hydrothermal precursor was obtained. The resulting

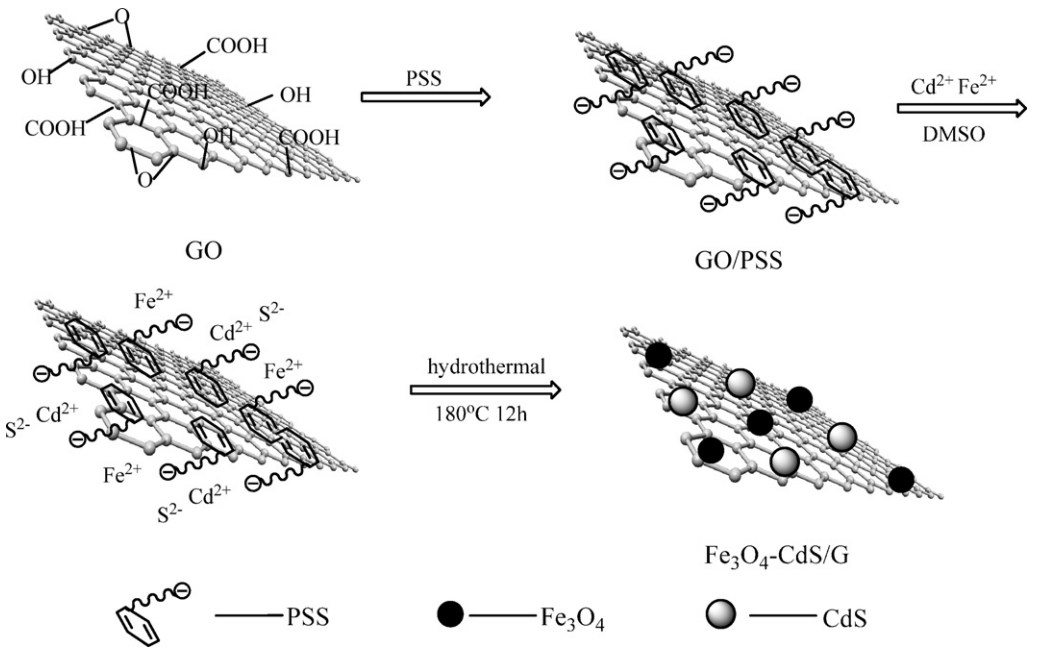

Fig. 1. Schematic diagram for the formation of Fe_3O_4-CdS/G nanocomposites.

precursor was then transferred into a Teflon-lined stainless steel autoclave (100 mL), and treated at 180 °C for 12 h. After that, the products were collected by magnet, repeatedly washed by acetone and absolute ethanol, then dried in a vacuum oven at 60 °C, the finally obtained products were Fe_3O_4-CdS/G nanocomposites.

2.3. Loading of Fe_3O_4-CdS/G nancomposites with doxorubicin (DOX)

Fe_3O_4-CdS/G nancomposites with a final concentration of 0.1 mg/mL and DOX with the certain concentration at pH 7.4 were first sonicated for 0.5 h and then stirred overnight at room temperature in the dark. All samples were ultracentrifuged at 14 000 rpm for 1 h. As comparison, GO was loaded with DOX under similar conditions.

2.4. Measurements

The morphology and structure of the product was observed by transmission electronic microscopy (TEM, Hitachi, Japan). The XRD spectrum was recorded using a Bruker D8 diffractometer with Cu Kα radiation (λ = 1.5418 Å) at a scanning rate of 0.02°/s and time step of 2 s with a 2θ ranging from 10 to 80°. A vibrating sample magnetometer (VSM, Yangzhou University Instrument Plant, LH-3) was used to measure the magnetic moment. Photoluminescence spectra was obtained on a F-96 spectrophotometer at room temperature. The DOX concentration in the upper layer was measured using a standard DOX concentration curve generated with an Ultraviolet-visible-near IR spectrophotometer (UV-VIS-NIR) (JASCO, V-570) at the wavelength of 233 nm from a series of DOX solutions with different concentrations.

3. Results and discussion

X-ray diffraction (XRD) characterization was conducted to obtain the structural information about Fe_3O_4-CdS/G nanocomposites (Fig. 2(a)). The XRD pattern of the as-prepared nanocomposites matches both the magnetite Fe_3O_4 (JCPDS card N° 19-0629) and CdS (JCPDS card N° 6-314). Six diffraction lines are observed in the representative XRD pattern of Fe_3O_4 at 2θ = 30.2°, 35.6°, 43.3°, 53.7°, 57.3° and 62.8°. These diffraction lines can be assigned to the (220), (311), (400), (422), (511), and (440) reflections, respectively, of the pure cubic spinel crystal structure of Fe_3O_4 with cell constant a = 8.39 Å [17]. And the six strong diffraction peaks can be assigned to the (100), (002), (101), (110), (103), and (112) crystal planes of the hexagonal CdS. Although the characteristic peak of GO located at 10.4° disappeared, the diffraction peak of graphene appeared, confirming the formation of graphene [18]. No impurity peak was observed, which indicated the high purity of the final products was successfully synthesized under current experimental conditions. Furthermore, the mean diameters of the Fe_3O_4 and CdS nanoparticles were determined to be 11.4 nm and 15.5 nm from the width of the strongest diffraction line (311) and (101) by using the Debye–Scherrer formula.

Transmission electron microscopy (TEM) image (Fig. 2(b)) displays the image of the as-prepared Fe_3O_4-CdS/G nanocomposites. It is noticeable that the graphene sheets are well-decorated by dense CdS and Fe_3O_4. Besides, the individual nanoparticles are well-separated from each other and distributed uniformly on the graphene, which is thought to be correlated with the existence of PSS on the surface of graphene. PSS possesses an abundant negative charge which can aid during dispersion and provide more nucleation sites for the formation of CdS and Fe_3O_4. Furthermore, the nanoparticle size was similar to that observed by XRD. The insert in Fig. 2(b) is a corresponding electron diffraction pattern revealing the satisfactory crystallinity of the sample, which can be indexed to the spinel structure of Fe_3O_4 as well as hexagonal CdS, which again provides evidence of Fe_3O_4-CdS/G nanocomposites formation.

Fluorescence spectra of the free CdS QDs and Fe_3O_4-CdS/G are shown in Fig. 3. Compared to the emission spectra of CdS QDs (519 nm), the band-edge emission spectra of Fe_3O_4-CdS/G blueshifts to 513 nm due to quantum confinement effect and a high concentration of

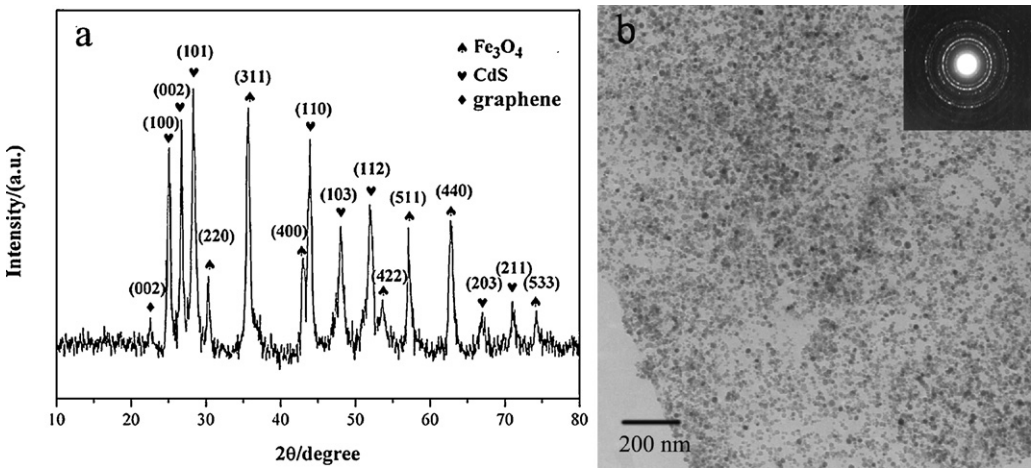

Fig. 2. (a) XRD pattern of Fe_3O_4-CdS/G nanocomposites. (b) TEM image of Fe_3O_4-CdS/G nanocomposites.

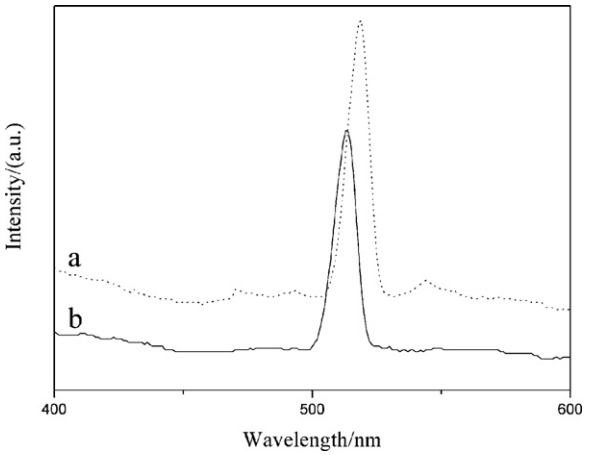

Fig. 3. Fluorescence spectra of (a) CdS and (b) Fe_3O_4-CdS/G nanocomposites.

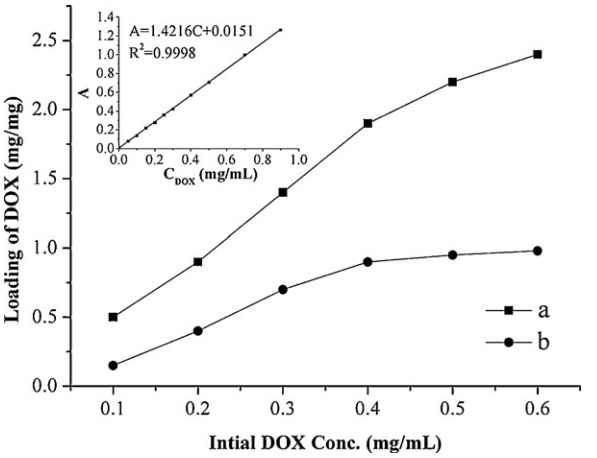

Fig. 5. Loading capacity of DOX on GO (a) and Fe_3O_4-CdS/G nancomposites (b) in different initial DOX concentrations. Inset: The linear relation curve between UV-absorption and concentrations of DOX.

point defects in the lattice. On the other hand, the low intensity surface defect emissions spectra of Fe_3O_4-CdS/G are completely quenched due to surface interactions of CdS QDs with graphene.

The magnetization curve of Fe_3O_4-CdS/G nanocomposites was measured at room temperature, as shown in Fig. 4. The magnetic hysteresis loop is S-like curve. The magnetic remanence of the sample is nearly zero. This indicates that there is almost no remaining magnetization when the external magnetic field was removed, suggesting that Fe_3O_4-CdS/G nanocomposites exhibit a superparamagnetic behavior. The saturation magnetization (Ms) of the sample is 44.85 emu/g. This value is smaller than the reported value of bulk Fe_3O_4 of 92 emu/g. This reduction in Ms may be attributed to the smaller size of the Fe_3O_4 nanoparticles and the relatively low amount of Fe_3O_4 loaded on graphene [19]. The magnetic property remained enough magnetic to meet the need of magnetic separation,

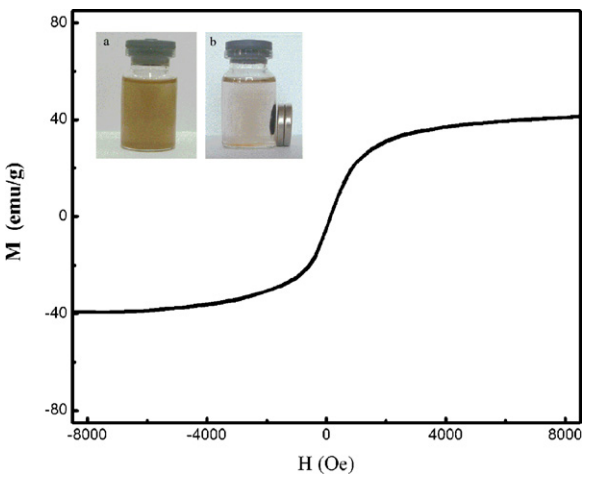

Fig. 4. Magnetization curve of Fe_3O_4-CdS/G nanocomposites. The top insert shows (a) a homogeneous dispersion of Fe_3O_4-CdS/G in the absence of an external magnetic field; (b) the good response of Fe_3O_4-CdS/G nanocomposites to a magnet.

as observed in Fig. 4b (top insert). In the absence of an external magnetic field, a homogeneous dispersion existed (Fig. 4a insert). When an external magnetic field was applied, the black particles were attracted to the vial wall in a short period of time. This reveals that the Fe_3O_4-CdS/G nancomposites have the potential for application in the field of targeted drug delivery.

The loading capacity of DOX on Fe_3O_4-CdS/G nancomposites was determined by UV spectrum at 233 nm, which was calculated by the difference of DOX concentrations between the original DOX solution and the supernatant solution after loading. The loading amount of DOX on Fe_3O_4-CdS/G nancomposites was investigated in different initial DOX concentrations with respect to the same concentration of Fe_3O_4-CdS/G nancomposites (0.1 mg/mL), and the loading of DOX on GO is used as a comparison, as shown in Fig. 5. The inset is the linear relation curve between UV-absorption and concentrations of DOX, and the correlation equation is $A = 1.4216C + 0.0151$ ($R^2 = 0.9998$). The absorbance of DOX has built up linearly ($R^2 = 0.9998$) with increasing concentration in the range of 0.05 mg/mL to 0.9 mg/mL. The saturated loading amount of DOX on Fe_3O_4-CdS/G is 0.98 mg/mg while the amount of DOX loaded on GO can reach 2.4 mg/mg at the DOX concentration of 0.6 mg/mL. Compared with GO, Fe_3O_4-CdS/G loaded less DOX and this may be due to some surface areas of GO have been occupied by Fe_3O_4 and CdS nanoparticles. However, the loading capacity of Fe_3O_4-CdS/G is still higher than that of the other common drug carrier materials, such as polymer micelles (0.6 mg/mg) [15a], hydrogel microparticles (0.5 mg/mg) [15b], liposomes (0.09 mg/mg) [15c], carbon nanohorns (0.2 mg/mg) [15d]. The above results show that Fe_3O_4-CdS/G nancomposites are indeed promising candidates for drug carrier applications.

4. Conclusion

In conclusion, we have developed a facile route for preparing Fe_3O_4-CdS/G nanocomposites by solvothermal

method. GO acted as not only precursor of graphene but also as the growth matrix for Fe_3O_4 and CdS. Furthermore, the DMSO acted as a sulphide source as well as reducing agent resulting in the formation of CdS and a reduction of GO to graphene. The resulting Fe_3O_4-CdS/G possesses high loading efficiency, good magnetic and fluorescent properties, which is desirable in various targeted drug delivery and fluorescent imaging fields.

Acknowledgements

This work was financially supported by the National Natural Science Foundation of China (authorization numbers: 20975056 and 81102411), Shandong (ZR2011BZ004 and ZR2011BQ005); JSPS and NSFC under the Japan-China Scientific Cooperation Program (21111140014); the Taishan Scholar Program of Shandong Province (TS20070711); and the National Key Basic Research Development Program of China (973 special preliminary study plan) (Grant n°: 2012CB722705).

References

[1] X. Yang, X. Zhang, Z. Liu, Y. Ma, Y. Huang, Y. Chen, J. Phys. Chem. C. 112 (2008) 17554.
[2] (a) Z. Liu, J.T. Robinson, X. Sun, H. Dai, J. Am. Chem. Soc. 130 (2008) 10876;
(b) X. Sun, Z. Liu, K. Welsher, J.T. Robinson, A. Goodwin, S. Zaric, H. Dai, Nano Res. 1 (2008) 203.
[3] N.A. Frey, S. Peng, K. Cheng, S.H. Sun, Chem. Soc. Rev. 38 (2009) 2532.
[4] (a) J. Shen, Y. Hu, M. Shi, N. Li, H. Ma, M. Ye, J. Phys. Chem. C. 114 (2010) 1498;
(b) H.P. Cong, J.J. He, Y. Lu, S.H. Yu, Small 6 (2010) 169;
(c) V.K. Singh, M.K. Patra, M. Manoth, G.S. Gowd, S.R. Vadera, N. Kumar, New Carbon Mater. 24 (2009) 147.
[5] T. Szabo, A. Bakandritsos, V. Tzitzios, E. Devlin, D. Petridis, I. Dekany, J. Phys. Chem. B. 112 (2008) 14461.
[6] F. He, J. Fan, D. Ma, L. Zhang, C. Leung, H. LaiwaChan, Carbon 48 (2010) 3139.
[7] H. He, C. Gao, Appl. Mater. Interfaces 2 (2010) 3201.
[8] (a) P. Lian, X. Zhu, H. Xiang, Z. Li, W. Yang, H. Wang, Electrochim. Acta 56 (2010) 834;
(b) X. Shen, J. Wu, S. Bai, H. Zhou, J. Alloy Compd. 506 (2010) 136.
[9] (a) X. Yang, X. Zhang, Y. Ma, Y. Huang, Y. Wang, Y. Chen, J. Mater. Chem. 19 (2009) 2710;
(b) V. Chandra, J. Park, Y. Chun, J.W. Lee, I. Hwang, K.S. Kim, ACS Nano 4 (2010) 3979.
[10] (a) M. Bruchez Jr., M. Moronne, P. Gin, S. Weiss, A.P. Alivisatos, Science 281 (1998) 2013;
(b) X. Michalet, F.F. Pinaud, L.A. Bentolila, J.M. Tsay, S. Doose, J.J. Li, G. Sundaresan, A.M. Wu, S.S. Gambhir, S. Weiss, Science 307 (2005) 538;
(c) I.L. Medintz, H.T. Uyeda, E.R. Goldman, H. Mattoussi, Nat. Mater 4 (2005) 435;
(d) A.M. Derfus, W.C.W. Chan, S.N. Bhatia, Adv. Mater. 16 (2004) 961.
[11] (a) A.A. Chen, A.M. Derfus, S.R. Khetani, S.N. Bhatia, Nucleic Acids Res. 33 (2005) e190;
(b) W.B. Tan, S. Jiang, Y. Zhang, Biomaterials 28 (2007) 1565;
(c) N. Jia, Q. Lian, H. Shen, C. Wang, X. Li, Z. Yang, Nano Lett. 7 (2007) 2976;
(d) D. Akin, J. Sturgis, K. Ragheb, D. Sherman, K. Burkholder, J.P. Robinson, A.K. Bhunia, S. Mohammed, R. Bashir, Nat. Nanotechnol. 2 (2006) 441.
[12] A. Cao, Z. Liu, S. Chu, M. Wu, Z. Ye, Z. Cai, Y. Chang, S. Wang, Q. Gong, Y. Liu, Adv. Mater. 22 (2010) 103.
[13] M. Feng, R. Sun, H. Zhan, Y. Chen, Nanotechnology 21 (2010) 075601.
[14] H. Chang, X. Lv, H. Zhang, J. Li, Electrochem. Commun. 12 (2010) 483.
[15] (a) Y. Chan, T. Wong, F. Byrne, M. Kavallaris, V. Bulmus, Biomacromolecules 9 (2008) 1826;
(b) F. Cavalieri, E. Chiessi, R. Villa, L. Vigano, N. Zaffaroni, M.F. Telling, G. Paradossi, Biomacromolecules 9 (2008) 1967;
(c) W.T. Sun, N. Zhang, A.G. Li, W.W. Zou, W.F. Xu, Int. J. Pharm. 353 (2008) 243;
(d) T. Murakami, K. Ajima, J. Miyawaki, M. Yudasaka, S. Iijima, K. Shiba, Mol. Pharm. 1 (2004) 399.
[16] W.S. Hummers Jr., R.E. Offeman, J. Am. Chem. Soc. 80 (1958) 1339.
[17] M. Zhang, D. Lei, X. Yin, L. Chen, Q. Li, Y. Wang, T. Wang, J. Mater. Chem. 20 (2010) 5538.
[18] C. Zhu, S. Guo, Y. Fang, S. Dong, ACS Nano 4 (2010) 2429.
[19] K. Jasuja, V. Berry, ACS Nano 3 (2009) 2358.